Supplemental information

Dnmt3a and Dnmt3b-decommissioned fetal enhancers are linked to kidney disease

Yuting Guan[1, †], Hongbo Liu[1, †], Ziyuan Ma[1], Szu-Yuan Li[1], Jihwan Park[1], Xin Sheng[1], Katalin Susztak[1,*]

[1]Department of Medicine, Renal Electrolyte and Hypertension Division, Department of Genetics, Perelman School of Medicine, University of Pennsylvania, Philadelphia, PA, USA, 19104

†These authors contributed equally to this work.

*Corresponding author:

Katalin Susztak, MD, PhD, MSc

12-123 Smilow Translational Research Center

3400 Civic Center Blvd

Philadelphia, PA 19104

+1(215)-898-2009

ksusztak@pennmedicine.upenn.edu

Table of Contents

Figure S1

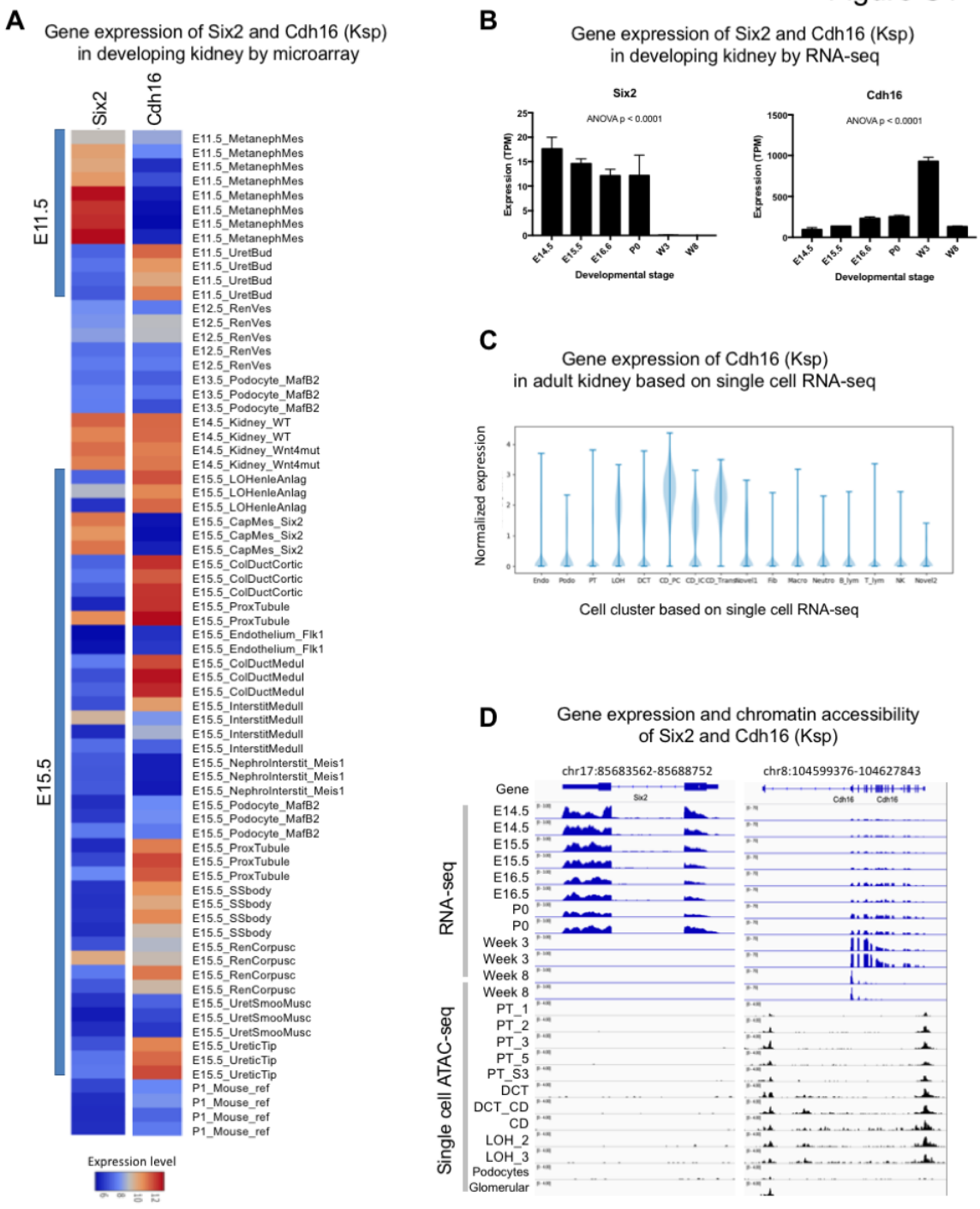

Figure S1. The spatial and temporal expression of *Six2* and *Cdh16* (*Ksp*) in the mouse kidney.

(**A**) Gene expression of *Six2* and *Cdh16* (*Ksp*) in developing kidney based on Affymetrix MOE430 microarray, obtained from GUDMAP database (https://www.gudmap.org/).

(**B**) RNA-seq based gene expression quantification of *Six2* and *Cdh16* (*Ksp*) in kidney development (https://www.encodeproject.org/).

(**C**) Gene expression of *Cdh16* (*Ksp*) in adult kidney based on single cell RNA-seq.

(**D**) Gene expression and chromatin accessibility of *Six2* and *Cdh16* (*Ksp*) in the developing and adult kidney (https://www.encodeproject.org). Single cell ATAC-seq data was obtained from Mouse sci-ATAC-seq Atlas (http://atlas.gs.washington.edu/mouse-atac/). Cell types was assigned to clusters by Cusanovich et al. as following: PT_1: Proximal tubule; PT_2: Proximal tubule; PT_3: Proximal tubule; PT_5: Proximal tubule; PT_S3: Proximal tubule S3; DCT: Distal convoluted tubule; DCT_CD: DCT/CD; CD: Collecting duct; LOH_2: Loop of henle; LOH_3: Loop of henle; Podocytes: Podocytes; Glomerular: Endothelial I (glomerular); and Macrophages. Genome intervals of gene loci in mm10 were converted to mm9 by lift-over and visualized by UCSC genome browser.

Figure S2

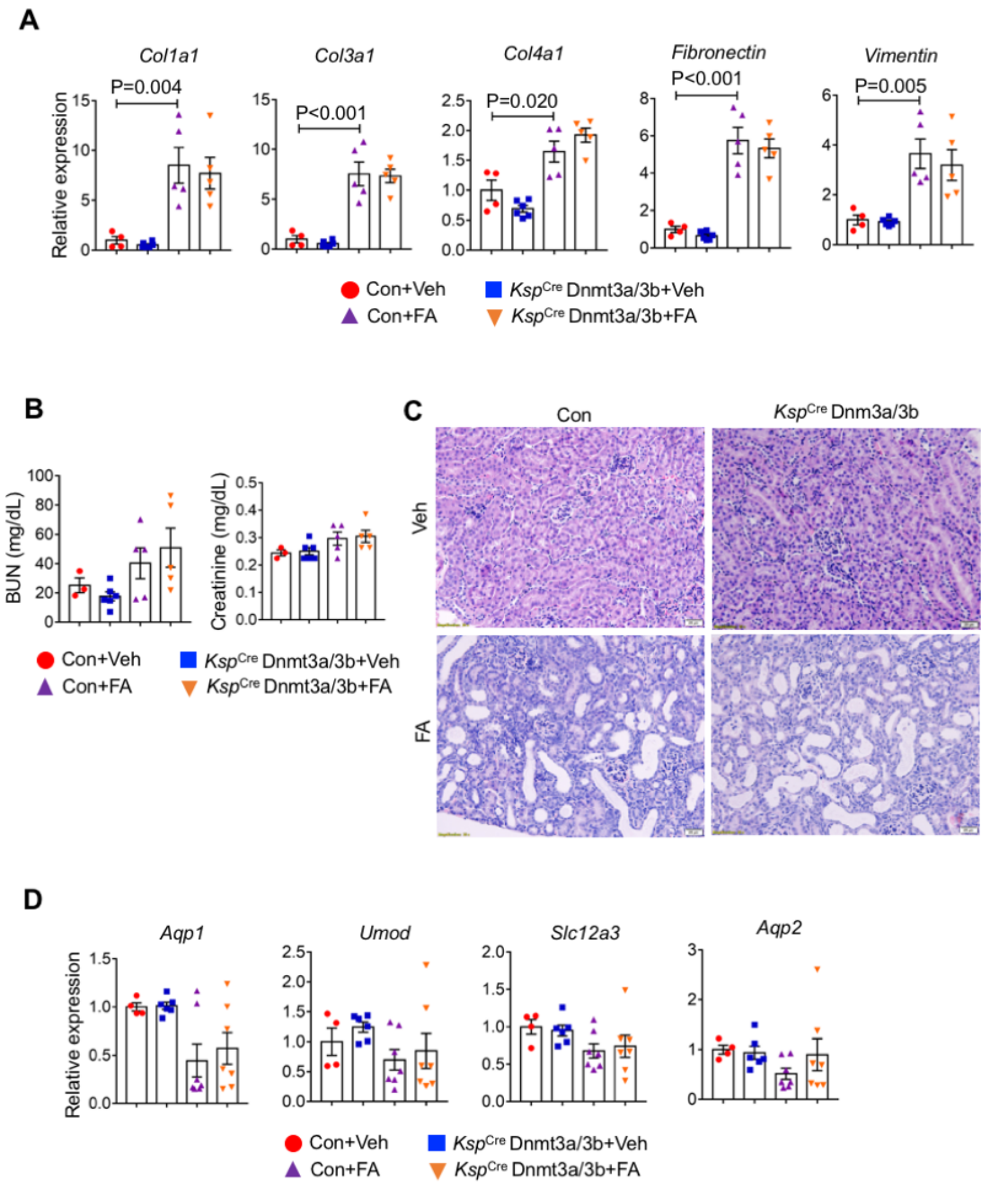

Figure S2. Effect of *Dnmt3a/3b* deletion in FA-induced kidney fibrosis model.

(**A**) Relative mRNA level of fibrosis associated genes *Col1a1*, *Col3a1*, *Col4a1*, *Fibronectin* and *Vimentin* in control and *Ksp*^{Cre}*Dnmt3a/3b* mice following sham or folic

acid treatment. Data are represented as mean ± SEM. P value was calculated by one-way ANOVA.

(**B**)Serum BUN and creatinine levels.

(**C**) Representative images of HE-stained kidney sections in control and *Ksp^{Cre}Dnmt3a/3b* following sham or folic acid treatment.

(**D**) Relative mRNA level of kidney segment marker genes *Aqp1*, *Umod*, *Slc12a3* and *Aqp2* in control and *Ksp^{Cre}Dnmt3a/3b* following sham or folic acid treatment. Data are represented as mean ± SEM.

Figure S3

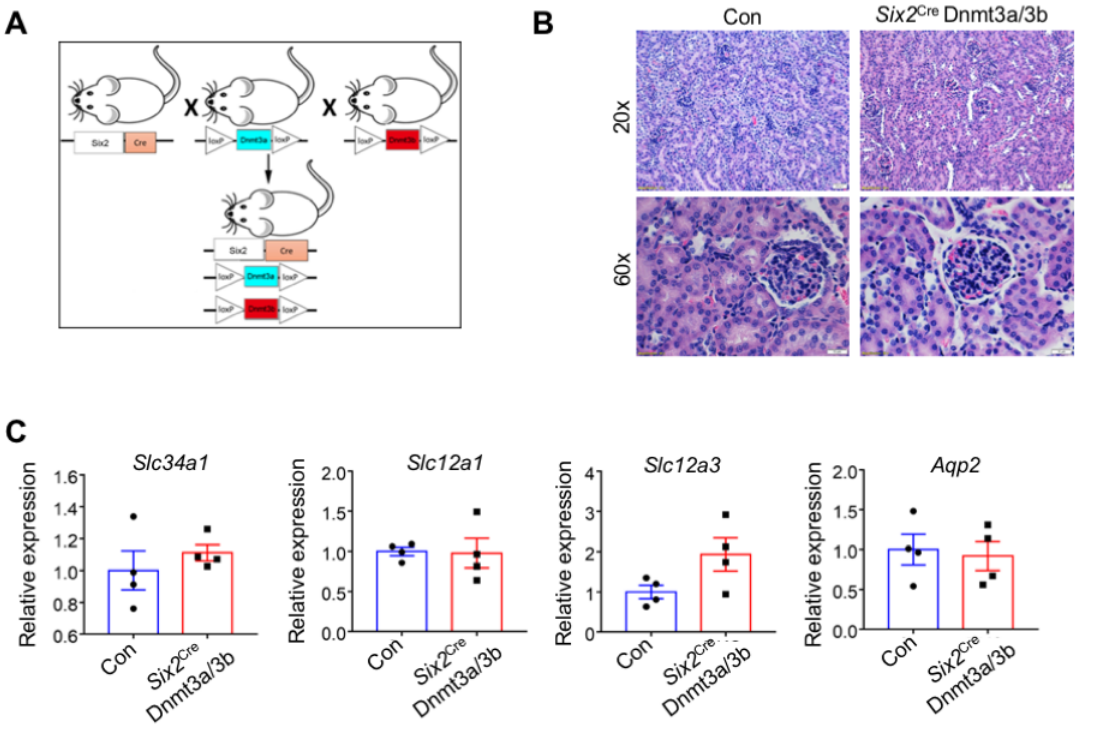

Figure S3. Phenotypic characterization of *Six2^{Cre}Dnmt3a/3b* mice

(A) Breeding scheme of generating *Six^{Cre}Dnmt3a/3b* double knock-out mice.

(**B**) Representative images of HE-stained kidney sections in control and *Six^{Cre}Dnmt3a/3b* mice. Scale bar: 50 μm.

(**C**) Relative mRNA level of kidney segment markers; such as *Slc34a1*, *Slc12a1*, *Slc12a3* and *Aqp2* in control and *Six^{Cre}Dnmt3a/3b* mice. Data are represented as mean ± SEM.

Figure S4

		Fraction of DMRs overlapped with				
DMR after Dnmt3a/b DKO	Total	CpG island	Kidney Promoter	Kidney Enhancer	Only Adult Kidney Enhancer	Only Fetal Kidney Enhancer
Ksp^{Cre} DKO Hyper-DMR	418	2.2%	8.9%	50.7%	3.1%	20.3%
Ksp^{Cre} DKO Hypo-DMR	1039	1.6%	8.1%	52.4%	0.0%	21.3%
Six2^{Cre} DKO Hyper-DMR	407	5.4%	11.5%	42.3%	3.7%	21.6%
Six2^{Cre} DKO Hypo-DMR	6777	2.4%	9.1%	56.7%	2.0%	26.9%

Figure S4. Genome location of DMRs induced by *Dnmt3a/3b* double knock-out.

CpG islands were downloaded from UCSC genome browser and chromatin states from fetal and adult kidneys were used to classify the genome location of each DMR.

Figure S5

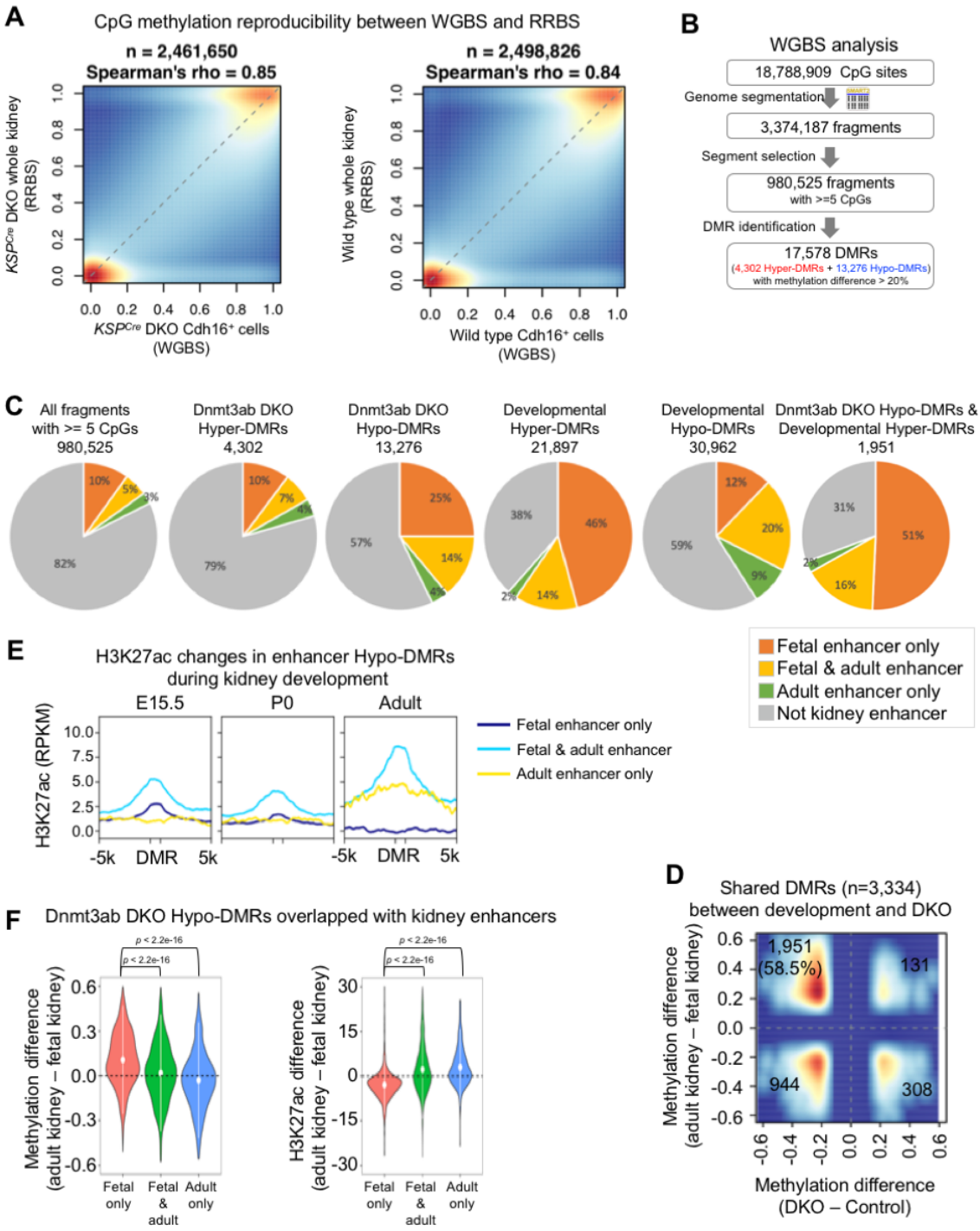

Figure S5. Cell-type specific base resolution methylation changes in *Ksp*^{Cre}*Dnmt3a/3b* mice.

(**A**) Reproducibility of CpG methylation by RRBS in whole kidney and that by WGBS in *Cdh16*$^{+}$ cell from kidney. Mice kidneys were harvested at 3 weeks after birth.

(**B**) WGBS analysis pipeline and DMR identification thresholds.

(**C**) Fraction of DMRs overlapping with enhancers in fetal and adult kidneys. Chromatin states from fetal and adult kidneys were used to classify the genome location of each DMR.

(**D**) Density plots of shared methylation changes of development and in *Dnmt3a/3b* knock-out mice. X-axis shows the methylation differences in *Dnmt3a/3b* knock-out and control mice; the y-axis shows the methylation changes of adult and fetal kidneys.

(**E**) Active enhancer (H3K27ac) enrichment of *Ksp*^{Cre}*Dnmt3a/3b* DMRs on E15.5, P0 and adult.

(**F**) Methylation differences in fetal or adult enhancers or enhancer that act as enhancers both in the adult and in the fetal kidneys.

Figure S6

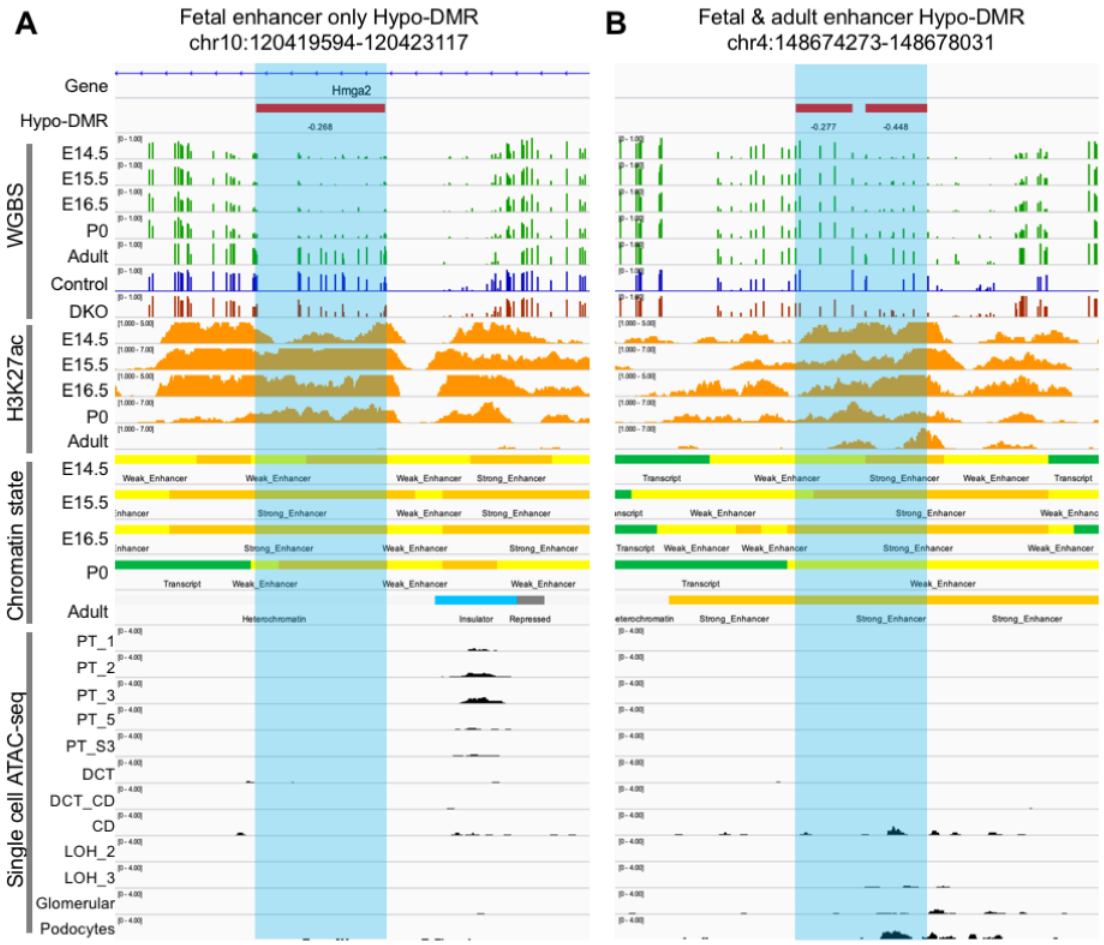

Figure S6. IGV genome browser of Hypo-DMR regions.

(**A**) IGV genome browser of the mouse chr10:120419594-120423117 and (**B**) chr4:148674273-148678031. Hypo DMRs were shown in red bar on the second track, followed by CpG methylation, H3K27ac, chromatin states during kidney development, and single cell open chromatin by single cell ATAC-Seq in adult kidney.

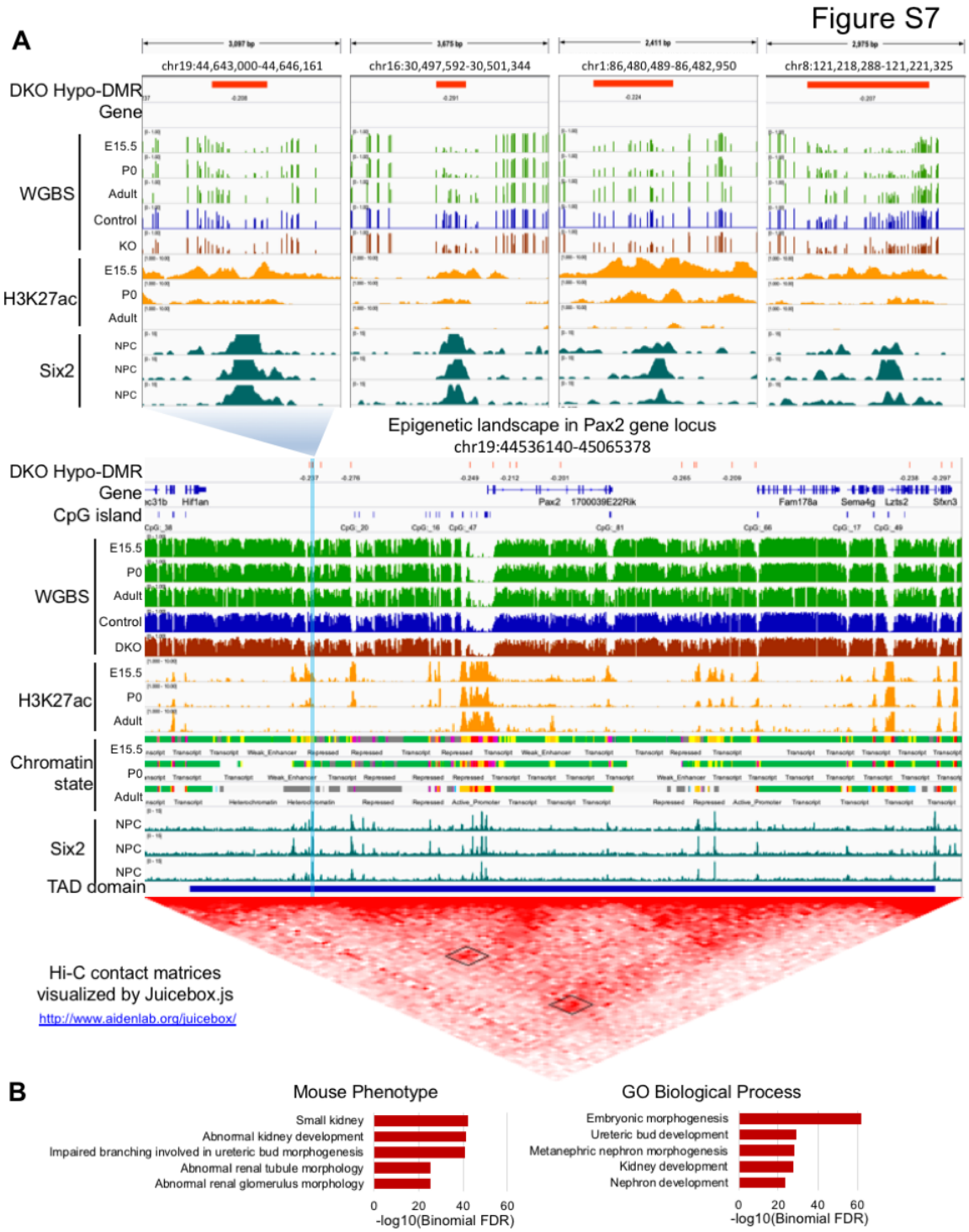

Figure S7. *Dnmt3a/3b* mediated methylation changes overlap with fetal enhancers and *Six2*-binding.

(**A**) IGV Genome browser view of four double knock-out hypo-DMRs (chr19:44643000-44646161, chr16:30497592-30501344, chr1:86480489-86482950, and chr8:121218288-121221325), followed by CpG methylation and H3K27ac during kidney development, and *Six2* binding sites by ChIP-seq in nephron progenitor cells (NPC). Bottom panel showed the IGV genome browser of mouse *Pax2* locus. Topologically associating domain (TAD) was defined in the genome of mouse ES-cells by Dixon et al. (Nature 2012). Hi-C contact matrices of data was detected by Kieffer-Kwon et al. (Molecular Cell 2017) and Juicebox.js (http://www.aidenlab.org/juicebox/) was to use for visualization.

(**B**) Biological processes and mouse phenotype enrichment around loci that gain methylation during development but not established in double knock-out kidneys, based on GREAT v3.0.0 (http://great.stanford.edu/great/public-3.0.0/html/).

Figure S8

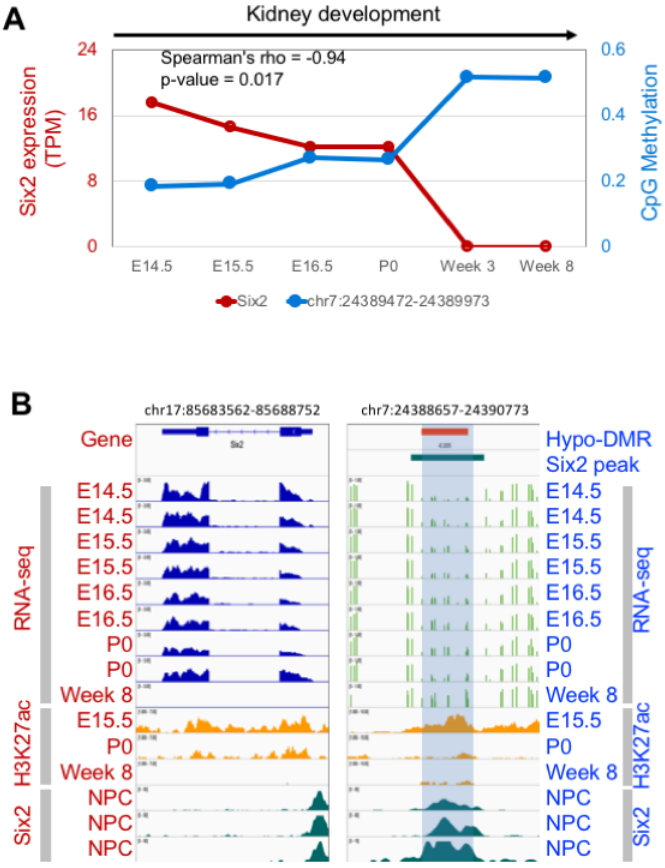

Figure S8. Correlation between methylation changes and *Six2* expression.

(**A**) Correlation between *Six2* expression and CpG methylation in a region on chromosome 7 (chr7:24389472-24389973) which showed strongest significant correlation with *Six2* expression.

(**B**) IGV genome browser of expression of *Six2* (left panel) and methylation of fragment (chr7:24389472-24389973, right panel) in kidney development. For both panels, enhancer mark H3K27ac and *Six2* peaks was shown in bottom tracks.

Figure S9

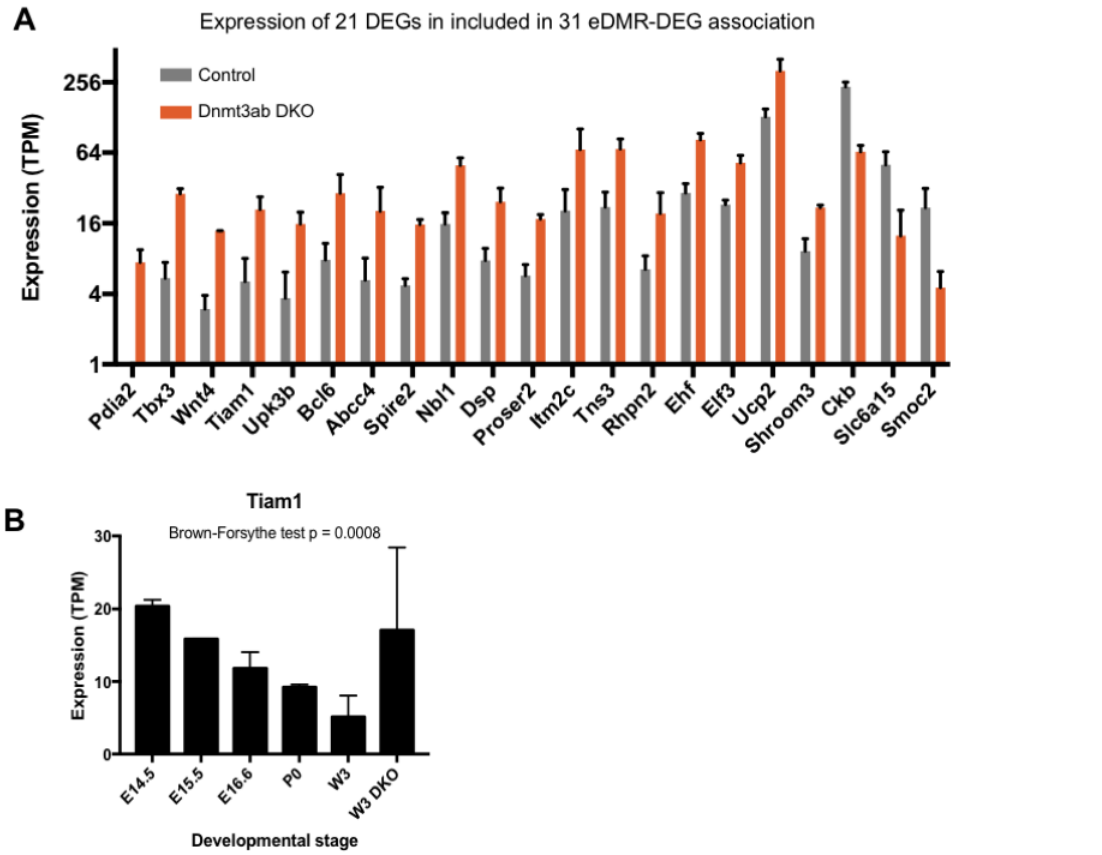

Figure S9. Methylation and gene expression correlation of topologically define enhancer DMRs and their target genes.

(**A**) Expression of 21 genes on control and *Dnmt3a*/*3b* double knock-out mice associated with topologically define enhancer methylation. Y-axis is the normalized expression level (Transcripts per million, TPM) detected by RNA-seq.

(**B**) *Tiam1* expression in the developing kidney and 3-week-old double knock-out mice.

Figure S10

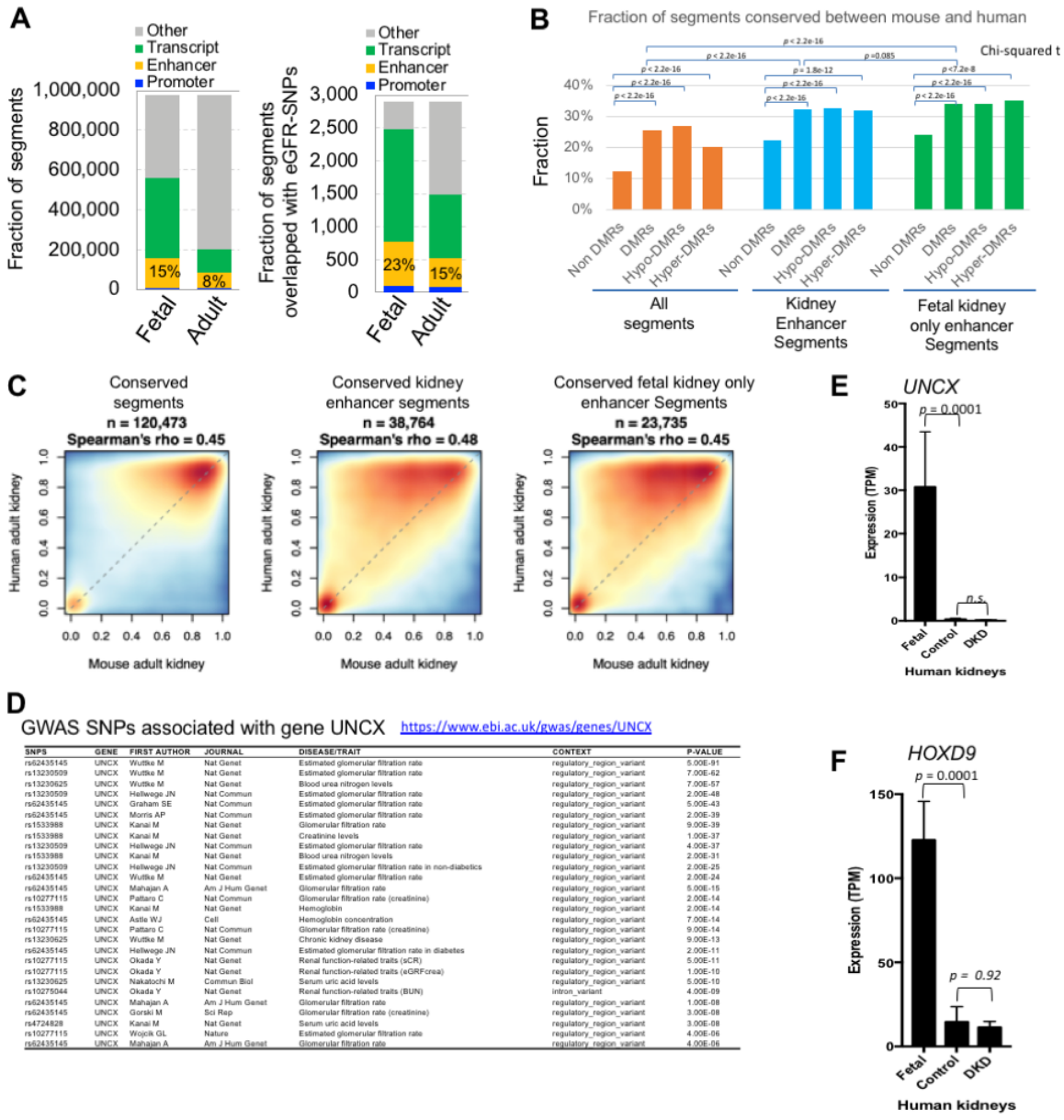

SNPS	GENE	FIRST AUTHOR	JOURNAL	DISEASE/TRAIT	CONTEXT	P-VALUE
rs62435145	UNCX	Wuttke M	Nat Genet	Estimated glomerular filtration rate	regulatory_region_variant	5.00E-91
rs13230509	UNCX	Wuttke M	Nat Genet	Estimated glomerular filtration rate	regulatory_region_variant	7.00E-62
rs13230625	UNCX	Wuttke M	Nat Genet	Blood urea nitrogen levels	regulatory_region_variant	7.00E-57
rs13230509	UNCX	Hellwege JN	Nat Commun	Estimated glomerular filtration rate	regulatory_region_variant	2.00E-48
rs62435145	UNCX	Graham SE	Nat Commun	Estimated glomerular filtration rate	regulatory_region_variant	5.00E-43
rs62435145	UNCX	Morris AP	Nat Commun	Estimated glomerular filtration rate	regulatory_region_variant	2.00E-39
rs1533988	UNCX	Kanai M	Nat Genet	Glomerular filtration rate	regulatory_region_variant	9.00E-39
rs1533988	UNCX	Kanai M	Nat Genet	Creatinine levels	regulatory_region_variant	1.00E-37
rs13230509	UNCX	Hellwege JN	Nat Commun	Estimated glomerular filtration rate	regulatory_region_variant	4.00E-37
rs1533988	UNCX	Kanai M	Nat Genet	Blood urea nitrogen levels	regulatory_region_variant	2.00E-31
rs13230509	UNCX	Hellwege JN	Nat Commun	Estimated glomerular filtration rate in non-diabetics	regulatory_region_variant	2.00E-25
rs62435145	UNCX	Wuttke M	Nat Genet	Estimated glomerular filtration rate	regulatory_region_variant	2.00E-24
rs62435145	UNCX	Mahajan A	Am J Hum Genet	Glomerular filtration rate	regulatory_region_variant	5.00E-15
rs10277115	UNCX	Pattaro C	Nat Commun	Glomerular filtration rate (creatinine)	regulatory_region_variant	2.00E-14
rs1533988	UNCX	Kanai M	Nat Genet	Hemoglobin	regulatory_region_variant	2.00E-14
rs62435145	UNCX	Astle WJ	Cell	Hemoglobin concentration	regulatory_region_variant	7.00E-14
rs10277115	UNCX	Pattaro C	Nat Commun	Glomerular filtration rate (creatinine)	regulatory_region_variant	9.00E-14
rs13230625	UNCX	Wuttke M	Nat Genet	Chronic kidney disease	regulatory_region_variant	9.00E-13
rs62435145	UNCX	Hellwege JN	Nat Commun	Estimated glomerular filtration rate in diabetes	regulatory_region_variant	2.00E-11
rs10277115	UNCX	Okada Y	Nat Genet	Renal function-related traits (sCR)	regulatory_region_variant	5.00E-11
rs10277115	UNCX	Okada Y	Nat Genet	Renal function-related traits (eGRFcrea)	regulatory_region_variant	1.00E-10
rs13230625	UNCX	Nakatochi M	Commun Biol	Serum uric acid levels	regulatory_region_variant	5.00E-10
rs10275044	UNCX	Okada Y	Nat Genet	Renal function-related traits (BUN)	intron_variant	4.00E-09
rs62435145	UNCX	Mahajan A	Am J Hum Genet	Glomerular filtration rate	regulatory_region_variant	1.00E-08
rs62435145	UNCX	Gorski M	Sci Rep	Glomerular filtration rate (creatinine)	regulatory_region_variant	3.00E-08
rs4724828	UNCX	Kanai M	Nat Genet	Serum uric acid levels	regulatory_region_variant	3.00E-08
rs10277115	UNCX	Wojcik GL	Nature	Estimated glomerular filtration rate	regulatory_region_variant	4.00E-06
rs62435145	UNCX	Mahajan A	Am J Hum Genet	Glomerular filtration rate	regulatory_region_variant	4.00E-06

Figure S10. Species conservation of kidney enhancers and their epigenetic changes in development and kidney disease.

(**A**) Genome location of all WGBS segments in fetal and adult kidneys. Chromatin states from fetal and adult kidneys were used to classify the genome location of each segment by WGBS.

(**B**) Fraction of segments conserved between mouse and human. All segments identified from WGBS dataset were classified according to their location relative to enhancer and methylation changes after *Dnmt3a/3b* double knock-out.

(**C**) CpG methylation of conserved segments in adult kidneys from mouse (8-week-old) and human (47.4±15.8 years old). Spearman's rank correlation coefficient and significance was calculated and showed.

(**D**) SNPs associated with gene UNCX obtained from GWAS catalog (https://www.ebi.ac.uk/gwas/genes/UNCX). Among total 40 terms, 68.3% (28 terms) were associated with kidney functions, and nearly all SNPs were localized in regulatory region of gene *UNCX*.

(**E-F**) Gene expression of *UNCX* and *HOXD9* in human fetal kidneys, normal adult kidneys and kidneys of patient with diabetic kidney disease (DKD). Transcripts per million (TPM) was used to quantify expression level. GraphPad Prism software (GraphPad Software Inc., La Jolla, CA) was used to plot and Dunnett's multiple comparisons test was used to calculate the significance of difference between normal adult human kidneys and fetal human kidneys and DKD kidneys.